

Application of an Undertow Model to Irregular Waves on Plane and Barred Beaches

Daniel T. Cox[†] and Nobuhisa Kobayashi[‡]

ABSTRACT

COX, D.T. and KOBAYASHI, N., 1998. Application of an Undertow Model to Irregular Waves on Plane and Barred Beaches. *Journal of Coastal Research*, 14(4), 1314-1324. Royal Palm Beach (Florida), ISSN 0749-0208.



An undertow model calibrated for regular waves on plane beaches is applied to predict the irregular wave induced undertow for both plane and barred beaches and for both laboratory and field data sets. The model combines a logarithmic profile in the bottom boundary layer with a conventional parabolic profile in the interior. The height and period of the irregular waves are represented by the local root-mean-square wave height and spectral peak period, and the measured mean volume flux below trough level is used as input to the model. The model is capable of predicting the undertow profiles both inside and outside the surf zone, provided that the empirical coefficient associated with the mean bottom shear stress is adjusted at each measuring line. The model appears to give reasonable predictions of the bottom boundary layer thickness and shear velocity, although these predictions could not be verified due to a lack of data. To develop a predictive undertow model, a simple relationship with an adjustable coefficient is applied to predict the measured volume flux below trough level using the local wave height and water depth. The calibration coefficients involved in the predictive model are not universal among the lab and field conditions possibly due to the effects of wave directionality and longshore currents in the field measurements, which are neglected in this paper.

ADDITIONAL INDEX WORDS: *Nearshore hydrodynamics, coastal engineering, analytical model, laboratory data, field data, undertow currents.*

INTRODUCTION

Detailed sediment transport models require accurate prediction of the cross-shore currents or undertow (e.g., ROELVINK and BROKER, 1993). Earlier work on analytical undertow models by DALLY and DEAN (1984), SVENDSEN (1984), STIVE and WIND (1986), and SVENDSEN *et al.* (1987) among others is based on the time-averaged, cross-shore momentum equation and verified primarily with laboratory measurements of the undertow induced by regular waves breaking on smooth, plane slopes. COX and KOBAYASHI (1996) showed the difficulties inherent in standard undertow models, including the difficulties in obtaining reliable estimates of all the terms in the time-averaged, cross-shore momentum equation. Furthermore, some of these models give no estimate of the undertow in the bottom boundary layer or the mean bottom shear stress. Recently, COX and KOBAYASHI (1997) developed a new undertow model without relying on the time-averaged momentum equation. They calibrated and verified the model using laboratory data of regular waves breaking on rough and smooth plane slopes. The model was found to give accurate predictions of the undertow profiles inside and outside the surf zone, provided that the empirical coefficient associated with the mean bottom shear stress was calibrated at each measuring line.

This paper extends their work by applying the model to predict undertow induced by irregular waves breaking over plane

and barred beaches using both laboratory and field data. Additionally, this paper shows how the mean volume flux below trough level, which is an input to the model, may be predicted from the local root-mean-square wave height and water depth. This paper is organized as follows. The model is briefly summarized, and the data sets used for comparison are discussed. Comparisons are then presented for undertow profiles and the mean volume flux below trough level along with a discussion of the calibration coefficients and model sensitivity. The performance of the model is summarized at the end with a discussion of the implications of the coefficients.

UNDERTOW MODEL

The undertow model presented by COX and KOBAYASHI (1997) is summarized herein to facilitate the comprehension of the subsequent comparisons. The model combines a conventional parabolic profile in the interior with a logarithmic profile in the bottom boundary layer where the logarithmic undertow profile in the bottom boundary layer has been verified using the data set of COX *et al.* (1996). The undertow \bar{u} from the bottom to trough level is expressed as

$$\bar{u} = \frac{\bar{u}_*}{\kappa} \ln\left(\frac{z_b}{z_0}\right) \quad \text{for } z_0 \leq z_b \leq \delta \quad (1)$$

and

$$\bar{u} = \bar{u}_b + \alpha z_b^2 \quad \text{for } \delta < z_b \leq d_t \quad (2)$$

where \bar{u}_* = mean shear velocity; κ = von Kármán constant, taken as $\kappa = 0.4$ in this paper; z_0 = bottom roughness height; z_b = vertical coordinate above the bottom, positive upward with $z_b = 0$ on the bottom; \bar{u}_b = hypothetical undertow ve-

97079 Received 12 June 1997; accepted in revision 5 January 1998.

[†] Ocean Engineering Program, Department of Civil Engineering, Texas A&M University, College Station, TX 77843, U.S.A.

[‡] Center for Applied Coastal Research, Department of Civil Engineering, University of Delaware, Newark, DE 19716, U.S.A.

Table 1. Summary of irregular wave induced undertow data for comparison with the undertow model.

Literature Cited	Data Set	Abbr.	Lab or Field	Bathymetry	tan α	H _{rms} (cm)	T _p (s)	\bar{h} (cm)	ξ
Sultan (1995)	Middle	S95	Lab	Plane, smooth	1:35	7.1	3.0	28.9	0.24
Okayasu and Katayama (1992)	Case 4	OK92	Lab	Barred, smooth	1:20	7.6	1.14	20.0	0.22
Smith <i>et al.</i> (1992)	901017	SSP92-A	Field	Barred, rough	1:22	59	9.7	230	0.38
Smith <i>et al.</i> (1992)	901018	SSP92-B	Field	Barred, rough	1:23	61	5.6	190	0.26
Smith <i>et al.</i> (1992)	901019	SSP92-C	Field	Barred, rough	1:28	65	7.0	221	0.25
Haines and Sallenger (1994)	Oct 11	HS94-A	Field	Barred, rough	1:22	99	13.3	145	0.32
Haines and Sallenger (1994)	Oct 12	HS94-B	Field	Barred, rough	1:18	101	14.4	200	0.44

locity in the absence of the boundary layer; δ = boundary layer thickness; d_t = water depth below trough level; and α = dimensional coefficient to be expressed in terms of the physical variables.

For smooth slopes typical of laboratory experiments, the roughness height is specified as z₀ = ν/(9ū*) based on unidirectional flow (e.g., SCHLICHTING, 1979) where ν is the kinematic viscosity. For rough slopes in the absence of bed forms, z₀ = 2 d₅₀/30 based on the analysis of regular waves breaking on a plane, rough slope where d₅₀ is the median grain diameter (COX *et al.*, 1996). Estimates of z₀ for the field data are more difficult due to the presence of ripples and megaripples and are explained later.

An expression for the mean shear velocity \bar{u}_* in (1) is developed using the quadratic friction equation for the temporal variation of the bottom shear stress τ_b given by

$$\tau_b = \frac{1}{2} \rho f_b |u_b| u_b \tag{3}$$

where ρ = fluid density; f_b = constant bottom friction factor; and u_b = instantaneous horizontal velocity at the bottom in the absence of the boundary layer. COX *et al.* (1996) showed that (3) could predict the measured temporal variation of τ_b within a factor of 2. For normally incident regular waves, u_b may be expressed as a sum of the sinusoidal wave component and the mean component \bar{u}_b and is given as

$$u_b = U_b \cos(kx - \omega t) + \bar{u}_b \tag{4}$$

where k = local wave number; x = horizontal coordinate, positive onshore; ω = angular wave frequency and t = time.

The amplitude U_b of the wave component in (4) is based on linear wave theory and is given as (e.g., JONSSON, 1966)

$$U_b = \frac{H\omega}{2 \sinh(k\bar{h})} \tag{5}$$

where H = local wave height, and \bar{h} = local water depth including the setup. Substituting (4) into (3) and taking the time-average with the assumption of a small current (\bar{u}_b/U_b)² ≪ 1, the mean bottom shear stress $\bar{\tau}_b$ may be given as

$$\bar{\tau}_b \approx \frac{2}{\pi} \rho f_b U_b \bar{u}_b \tag{6}$$

Defining the mean shear velocity by $|\bar{u}_*| \bar{u}_* = \bar{\tau}_b/\rho$ together with (6) yields

$$\bar{u}_* = (C_* f_b U_b |\bar{u}_b|)^{1/2} \frac{\bar{u}_b}{|\bar{u}_b|} \tag{7}$$

in which C* = empirical coefficient calibrated later. It is noted that C* ≈ 2/π if (3) and linear wave theory are accurate enough to estimate the relatively small value of \bar{u}_* , and it is further noted that the time-averaged bottom boundary layer is much less understood than the oscillatory bottom boundary layer (e.g., GRANT and MADSEN, 1986; NIELSEN, 1992).

The bottom friction factor f_b in (7) may be estimated for rough slopes as (JONSSON, 1966)

$$\frac{1}{4\sqrt{f_b}} + \log \frac{1}{4\sqrt{f_b}} = \log \left(\frac{A_b}{k_s} \right) - 0.08 \tag{8}$$

and for smooth slopes as (KAMPHUIS, 1975)

Table 2. Model input and calibration coefficients for S95.

Line No.	d (cm)	H _{rms} (cm)	$\bar{\eta}$ (cm)	η _{lr} (cm)	Q _t (cm ² /s)	\bar{h}	U _b (cm/s)	Re × 10 ⁻⁴	f _b × 10 ⁻²	C	C _f	C _u
S1	29.0	7.1	-0.11	-3.2	-49	0.367	19.8	1.6	1.4	0.060	1.2	1.5
S2	23.3	8.1	-0.15	-2.6	-44	0.327	25.5	2.7	1.2	0.060	1.3	0.9
S3	20.8	8.6	-0.17	-1.8	-45	0.308	28.8	3.4	1.1	0.060	1.3	0.8
S4	17.7	8.6	-0.16	-1.9	-39	0.283	31.4	4.1	1.1	0.060	1.3	0.6
S5	16.1	8.1	-0.14	-2.1	-46	0.271	31.0	4.0	1.1	0.060	1.2	0.8
S6	14.4	7.2	-0.13	-2.1	-36	0.256	29.2	3.5	1.1	0.070	1.1	0.8
S7	13.1	6.5	-0.09	-1.5	-44	0.243	27.8	3.2	1.2	0.080	1.0	1.1
S8	12.1	6.1	-0.01	-1.2	-41	0.229	27.6	3.2	1.2	0.090	1.0	1.1
S9	9.7	5.3	0.09	-1.3	-45	0.209	26.3	2.9	1.2	0.110	1.8	1.5
S10	7.7	4.2	0.23	-1.0	-29	0.186	23.5	2.3	1.3	0.120	1.8	1.5
S11	5.6	3.3	0.40	-1.1	-25	0.164	21.0	1.8	1.4	0.130	1.7	1.9
S12	3.1	1.7	0.66	0.0	-16	0.128	13.8	0.8	1.7	0.170	1.6	3.4

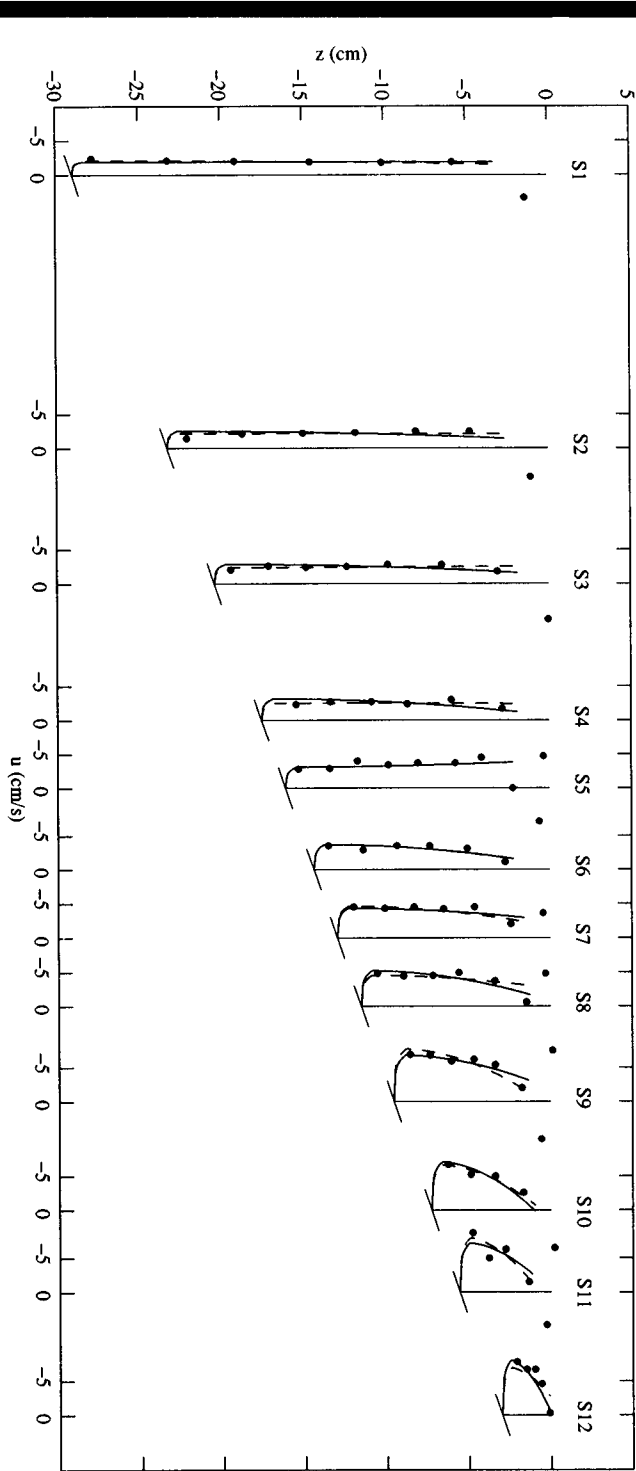


Figure 1. Model predictions for S95: Measured \bar{u} (●); Predicted, Method 1 (—); and Predicted, Method 2 (---).

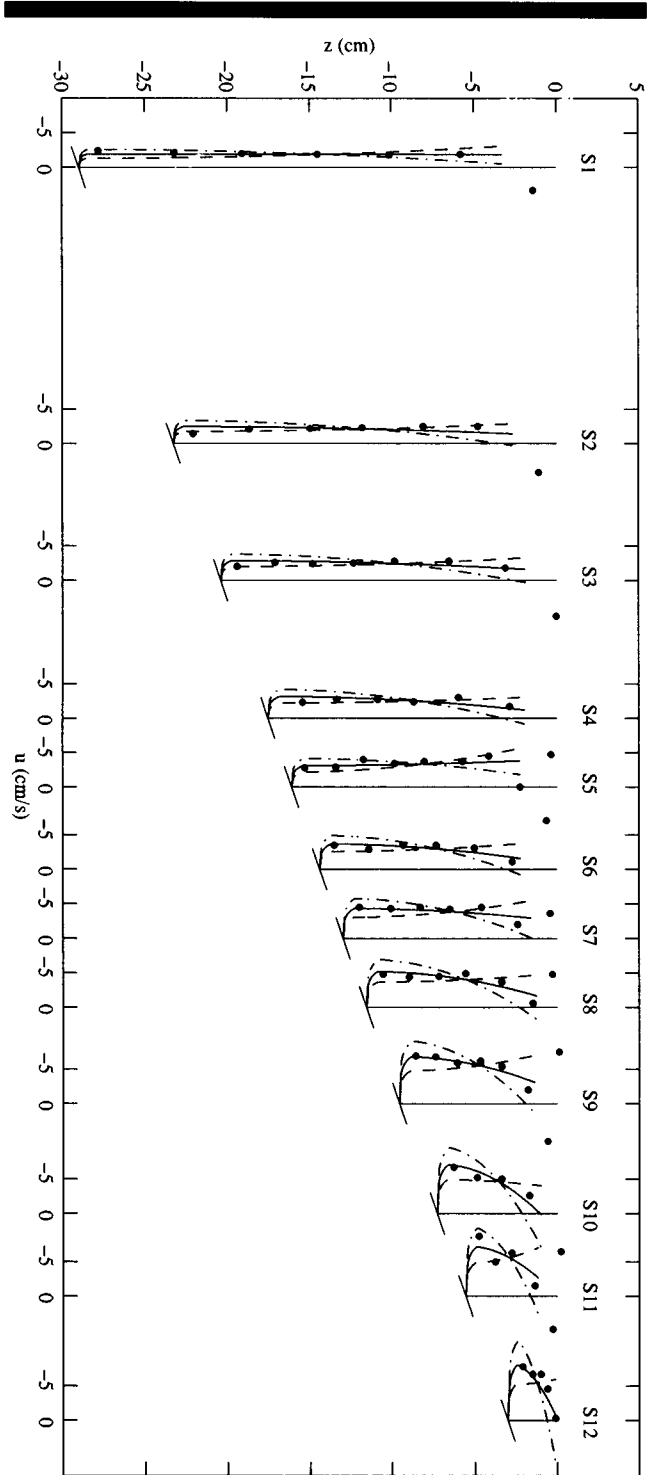


Figure 2. Model sensitivity for S95: Measured \bar{u} (●); Predicted, Method 1 with adopted C , (—); Predicted, Method 1 with $0.8 C$, (---); and Predicted, Method 1 with $1.2 C$, (-·-).

Table 3. Model input and calibration coefficients for OK92.

Line No.	d (cm)	H_{rms} (cm)	$\bar{\eta}$ (cm)	η_r (cm)	Q_t (cm ² /s)	$k\bar{h}$	U_b (cm/s)	$Re \times 10^{-4}$	$f_b \times 10^{-2}$	C	C_f	C_u
O1	20.0	5.4	0.00	-2.0	-6	0.878	14.9	0.4	2.3	0.030	2.0	0.3
O2	12.0	5.5	0.07	-1.7	-17	0.649	21.7	0.7	1.8	0.050	1.3	0.6
O3	8.0	5.2	0.12	-1.5	-17	0.523	25.9	1.1	1.6	0.060	1.1	0.6
O4	10.0	3.7	0.24	-1.1	-18	0.591	16.3	0.4	2.2	0.100	1.0	1.2
O5	10.0	3.6	0.29	-1.1	-4	0.593	15.9	0.4	2.2	0.040	1.7	0.3
O6	6.0	3.9	0.21	-1.2	-7	0.453	22.8	0.8	1.7	0.060	1.3	0.4

$$\frac{1}{8.1\sqrt{f_b}} + \log \frac{1}{\sqrt{f_b}} = \log \sqrt{Re} - 0.135 \tag{9}$$

where A_b = excursion amplitude given by $A_b = U_b/\omega$; k_s = equivalent roughness taken as $k_s = 30 z_0$; and Re = Reynolds number defined as $Re = U_b A_b/\nu$. COX *et al.* (1996) showed that (8), which was developed for nonbreaking waves, could predict the value of f_b within a factor of 2 even inside the surf zone for their rough slope experiment.

Assuming that the thickness of the undertow boundary layer is approximately equal to the thickness of the wave boundary layer, the boundary layer thickness δ in (1) and (2) may be approximated by (GRANT and MADSEN, 1979)

$$\delta = C_\delta \frac{\kappa(u_*)_{max}}{\omega} \tag{10}$$

where $(u_*)_{max}$ = maximum shear velocity over the wave period; and C_δ = empirical constant in the range $1 \leq C_\delta \leq 2$ and is taken as $C_\delta = 1.5$ in this paper because the predicted results have been found to be insensitive to C_δ in this range. The maximum shear velocity $(u_*)_{max}$ in (10) is estimated by taking the maximum of (3) using (4) and employing the small current assumption used to derive (7). Substitution of this expression into (10) yields

$$\delta = C_\delta \left(\frac{\kappa}{\omega} \right) \left[\frac{1}{2} f_b U_b (U_b + 2|\bar{u}_b|) \right]^{1/2} \tag{11}$$

The coefficient α in (2) can be obtained by matching (1) and (2) at $z_b = \delta$ which yields

$$\alpha = \frac{1}{\delta^2} \left[\frac{\bar{u}_*}{\kappa} \ln \left(\frac{\delta}{z_0} \right) - \bar{u}_b \right] \tag{12}$$

To close the problem, the mean volume flux below trough level, Q_t , is specified and is estimated from the measured undertow profile in this paper. The prediction of Q_t will be addressed separately at the end of this section. The volume flux is defined as

$$Q_t = \int_{z_0}^{d_t} \bar{u} dz_b \tag{13}$$

where Q_t is negative for the undertow \bar{u} . Substituting (1) and (2) into (13) and solving for \bar{u}_b gives

$$\bar{u}_b = \frac{1}{d_t} \left[Q_t + \frac{\bar{u}_*}{\kappa} \delta - \frac{\alpha}{3} (d_t^3 + 2\delta^3) \right] \tag{14}$$

The solution of (1), (2), (7), (11), and (12) with (14) is termed Method 1.

In light of the uncertainty in estimating the relatively small \bar{u}_* using the time-averaging of the quadratic equation (3), a second method is proposed to estimate \bar{u}_* directly from \bar{u}_b without regard to the oscillatory wave velocity. Instead of (7), \bar{u}_* is assumed to be expressed as

$$|\bar{u}_*| \bar{u}_* = \frac{1}{2} \bar{f} |\bar{u}_b| \bar{u}_b \tag{15}$$

in which \bar{f} = empirical friction factor for the undertow assumed to be given by $\bar{f} = C_f f_b$ where C_f is an empirical coefficient. It is noted that $C_f = 1$ if the friction factors \bar{f} and f_b for the undertow and wave induced velocity are the same. From (15), the mean shear velocity is given by

$$\bar{u}_* = \sqrt{0.5 C_f f_b} \bar{u}_b \tag{16}$$

Since (16) does not require the small current assumption used in (7), $(\tau_b)_{max}$ is derived from (3) without this assumption and is given as

$$(\tau_b)_{max} = \rho [(u_*)_{max}]^2 = \frac{1}{2} \rho f_b (U_b + |\bar{u}_b|)^2 \tag{17}$$

Substitutions of (17) into (10) for the boundary layer thickness gives

$$\delta = C_\delta \left(\frac{\kappa}{\omega} \right) \sqrt{\frac{f_b}{2}} (U_b + |\bar{u}_b|) \tag{18}$$

In short, \bar{u}_* and δ estimated by (7) and (11) in Method 1 are replaced by (16) and (18) in Method 2. Since C_δ is fixed, each method has only one primary calibration coefficient: C_* for Method 1 and C_f for Method 2. These methods may not be satisfactory physically, but they are necessary to estimate the mean shear velocity \bar{u}_* whose data appears to be limited, especially inside the surf zone.

The above undertow model developed originally for normally-incident regular waves may also be applied to normally-incident irregular waves by approximating the irregular waves by the equivalent regular waves based on the local root-mean-square wave height, H_{rms} , and the spectral peak period, T_p . The use of H_{rms} may be appropriate because the mean volume flux Q_t given by (13) is approximately proportional to the square of the local wave height as explained below. The choice of the spectral peak period is somewhat arbitrary, but this period is typically reported for irregular wave data. For field data, the cross-shore fluid motion under directional random waves may be approximated by that under normally-incident random waves if $\theta_c^2 \ll 1$ where θ_c is the characteristic incident angle in radians (KOBAYASHI and

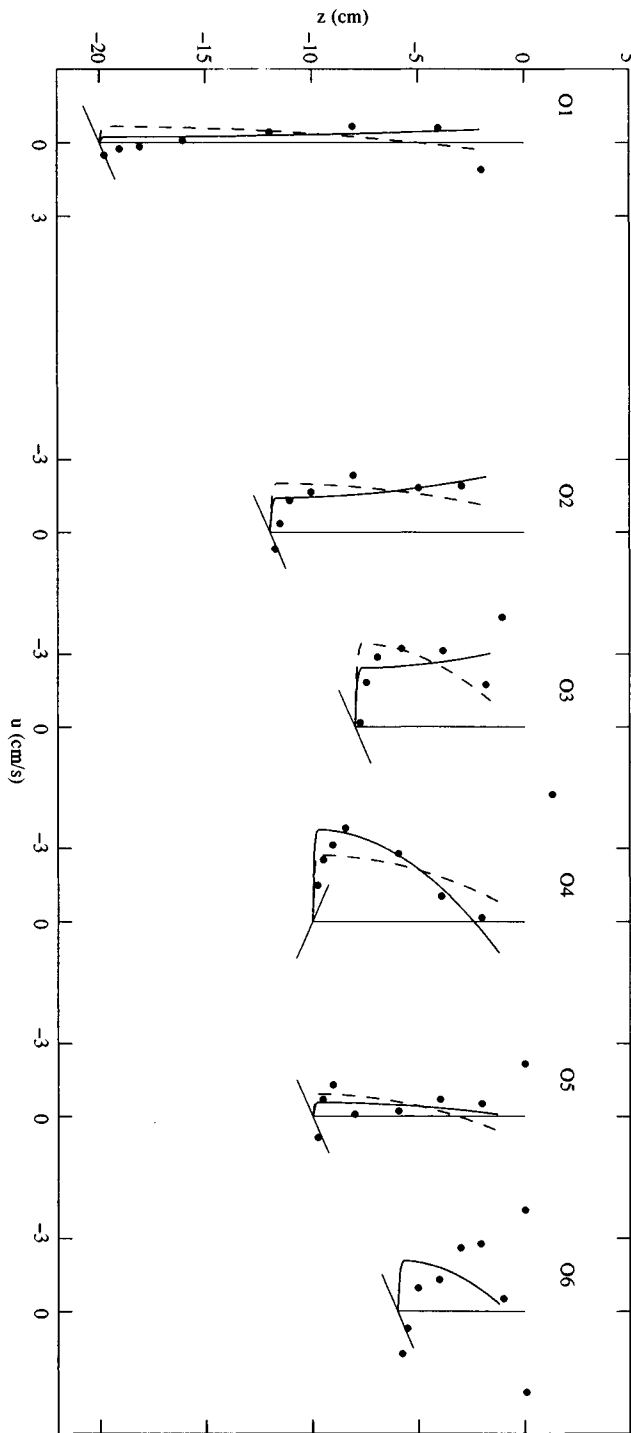


Figure 3. Model predictions for OK92: Measured \bar{u} (●); Predicted, Method 1 (—); and Predicted, Method 2 (- -).

KARJADI, 1996). The assumption of $\theta_c^2 \ll 1$ is usually satisfied in the surf zone because of wave refraction. However, long-shore currents may not be negligible even if $\theta_c^2 \ll 1$ and may affect the mean cross-shore bottom shear stress in view of the

cross-shore sediment transport analysis using field data by THORNTON *et al.* (1996). Consequently, the subsequent comparisons with field data will need to be interpreted bearing this limitation in mind.

The use of the measured volume flux Q_t below trough level implies that this undertow model predicts the undertow profile but can not be used to predict the magnitude of the undertow. To address this shortcoming, an attempt is made to estimate Q_t from the local root-mean-square wave height, H_{rms} , and local water depth, $\bar{h} = (d + \bar{\eta})$, where d = still water depth and $\bar{\eta}$ = setup. The volume flux below trough level is approximated as

$$Q_t \approx \bar{U} d_t \tag{19}$$

where \bar{U} = depth-averaged velocity estimated by

$$\bar{U} \approx -\frac{C_u \sqrt{g\bar{h}} (H_{rms})^2}{8 \bar{h}} \tag{20}$$

where g = gravitational acceleration, and C_u = empirical coefficient introduced herein to account for the roller effect. The roller effect is expected to increase the magnitude of \bar{U} inside the surf zone (SVENDSEN, 1984). KOBAYASHI *et al.* (1998) derived (20) with $C_u = 1$ from the time-averaged continuity equation together with the assumption of linear progressive long waves where H_{rms} is defined as $H_{rms} = \sqrt{8}\sigma$ with σ = standard deviation of the free surface elevation. It is further noted that cross-shore variation in wave height and setup could be predicted using the time-averaged equations for momentum and energy (e.g., BATTJES and JANSSEN, 1978; BATTJES and STIVE, 1985).

SUMMARY OF DATA SETS

Table 1 summarizes the data sets used for comparison with the undertow model, indicating the literature cited, the data set name from each paper, and the abbreviation used in this paper. The data are comprised of both laboratory and field conditions, and the undertow is induced by irregular waves for all cases. The sixth through ninth columns indicate the quantities used to compute the surf similarity parameter given by

$$\xi = \frac{\tan \alpha}{\sqrt{H_{rms}/L_p}} \tag{21}$$

where α = local beach slope, and L_p = local wavelength computed using linear wave theory with the peak period, T_p . For the first five cases, ξ is estimated at the most seaward measuring line as shown in the subsequent figures. For the last two cases, ξ is estimated at the fifth measuring line since the first four seaward measuring lines had a very gentle slope. The range of the surf similarity parameter for the seven cases listed in Table 1 is $0.22 \leq \xi \leq 0.44$, indicating spilling and plunging waves with little reflection of wind waves (BATTJES, 1974). It is noted that the definition of H_{rms} for these data sets was not clearly stated in all cases. As a result, the values of H_{rms} based on the standard deviation σ , the spectral method, and the zero-crossing method are assumed to be the same.

COX and KOBAYASHI (1997) compared the undertow model to the measured undertow induced by regular waves on plane

Table 4. Model input and calibration coefficients for SSP92-A,B,C.

Line No.	d (cm)	H_{rms} (cm)	$\bar{\eta}$ (cm)	η_{tr} (cm)	Q_t (cm ² /s)	$\bar{k}h$	U_b (cm/s)	A_b/k_s	$Re \times 10^{-5}$	$f_b \times 10^{-2}$	C_s	C_f	C_u
A1	230	59	0.0	-17	-0.23	0.319	59	61	5.4	2.7	0.020	0.25	2.7
A2	161	55	0.0	-16	-0.29	0.266	66	68	6.7	2.6	0.060	0.24	3.5
A3	106	47	0.0	-14	-0.24	0.215	71	73	7.8	2.5	0.060	0.24	3.3
A4	127	44	0.0	-13	-0.08	0.235	60	62	5.6	2.7	0.030	0.24	1.3
A5	167	44	0.0	-13	-0.08	0.271	52	53	4.2	2.8	0.020	0.23	1.3
A6	189	44	0.0	-13	-0.06	0.288	49	51	3.7	2.9	0.010	0.23	1.2
B1	190	61	0.0	-18	-0.18	0.515	64	38	3.6	3.4	0.020	0.21	1.9
B2	126	54	0.0	-16	-0.26	0.413	71	42	4.5	3.2	0.050	0.21	2.9
B3	92	43	0.0	-13	-0.15	0.351	67	41	4.1	3.3	0.050	0.20	2.3
B4	128	42	0.0	-13	-0.08	0.417	54	32	2.6	3.6	0.020	0.21	1.5
B5	156	42	0.0	-13	-0.02	0.463	48	29	2.1	3.8	0.010	0.21	0.5
B6	171	56	0.0	-17	-0.01	0.486	63	37	3.5	3.4	0.010	0.22	0.2
C1	221	65	0.0	-20	-0.17	0.439	65	48	4.7	3.0	0.020	0.23	1.6
C2	150	56	0.0	-17	-0.33	0.358	69	51	5.3	2.9	0.060	0.22	3.7
C3	105	49	0.0	-15	-0.27	0.298	73	54	5.9	2.8	0.060	0.22	3.4
C4	130	48	0.0	-14	-0.21	0.333	63	47	4.4	3.0	0.040	0.22	2.9
C5	169	45	0.0	-13	-0.06	0.381	51	38	2.9	3.4	0.020	0.21	0.9
C6	192	52	0.0	-16	-0.07	0.408	56	41	3.5	3.2	0.010	0.22	1.0

slopes in the laboratory. The first extension of this paper is to compare the model to laboratory undertow data for irregular waves on a plane slope (SULTAN, 1995), and then for irregular waves on a triangular barred profile (OKAYASU and KATAYAMA, 1992). These laboratory tests were for normally incident irregular waves with no longshore current. The next extension is to compare the model to the field data of SMITH *et al.* (1992) and HAINES and SALLENGER (1994). The field measurements were collected on a barred beach at the USACE Field Research Facility in Duck, North Carolina, under a fairly uniform bathymetry in the longshore direction (e.g., SMITH *et al.*, 1992). Although the longshore current was not reported in SMITH *et al.* (1992), the peak incident wave angle measured counter-clockwise from shore normal was given as $\theta = -15, -43, \text{ and } +24$ degrees at 8 m depth for SSP92-A, SSP92-B, and SSP92-C. Nevertheless, SMITH *et al.* (1992) compared their undertow model for essentially normally-incident waves with these data sets apart from an empirical correction of $\cos \theta$ in (20) with $C_u = 2.4$.

HAINES and SALLENGER (1994) reported the magnitude and direction of the longshore current for HS94-A and HS94-B. For HS94-A, the magnitude of the longshore current was generally less than the cross-shore current, but the longshore current was not unidirectional. For HS94-B, the magnitude of the longshore current was approximately on the same order as the cross-shore current and was unidirectional. HAINES and SALLENGER (1994) compared their undertow

model for normally-incident waves with their data sets, excluding one data set with vigorous longshore currents. It is noted that none of the data sets mentioned above included detailed measurements of the undertow and shear stress in the bottom boundary layer.

UNDERTOW PROFILES

The undertow model is compared with the seven data sets listed in Table 1 using the measured volume flux below trough level to close the system of equations as described above. The volume flux is estimated by integrating a cubic spline fitted through the measured points. For both Method 1 and Method 2, the calibration coefficients are adjusted at each measuring line to give a best fit "by eye" to the data as was done in COX and KOBAYASHI (1997) for the regular wave comparisons.

Table 2 lists the input parameters to the model at each measuring line for the data of SULTAN (1995) where $\eta_{tr} =$ negative trough elevation relative to the still water level which is used to calculate $d_t = (d + \eta_{tr})$. Since the trough level η_{tr} was not given in SULTAN (1995), η_{tr} was taken as the elevation where the undertow changed sign from negative to positive below the still water level. This elevation corresponds roughly to $0.3 H_{rms}$; and it is noted that the ratio of $|\eta_{tr}/H| \approx 0.3$ was found for the regular wave data of COX *et al.* (1996), NADAOKA and KONDOH (1982), and HANSEN and SVENDSEN (1984). Column 8 indicates the amplitude of the orbital velocity U_b based on linear wave theory; and for the cases presented here, the small current assumption $(\bar{u}_b/U_b)^2 \ll 1$ used in (6) is reasonable. Column 9 gives the Reynolds number used to estimate the friction factor f_b in Column 10 using (9) for the smooth slope, which are in the range $0.8 \times 10^4 \leq Re \leq 4.1 \times 10^4$ and $0.011 \leq f_b \leq 0.017$.

Columns 11 and 12 give the calibration coefficients C_s for Method 1 and C_f for Method 2. C_s increases shoreward as was found in COX and KOBAYASHI (1997) for the regular wave comparisons, but the variation in C_s from outside the surf

Table 5. Average values of C_s , C_f and C_u for SSP92-A, B, and C.

Line No.	$C_{s,ave}$	$C_{f,ave}$	$C_{u,ave}$
1	0.020	0.230	2.07
2	0.057	0.220	3.37
3	0.057	0.217	3.00
4	0.030	0.220	1.90
5	0.017	0.217	0.90
6	0.010	0.227	0.80

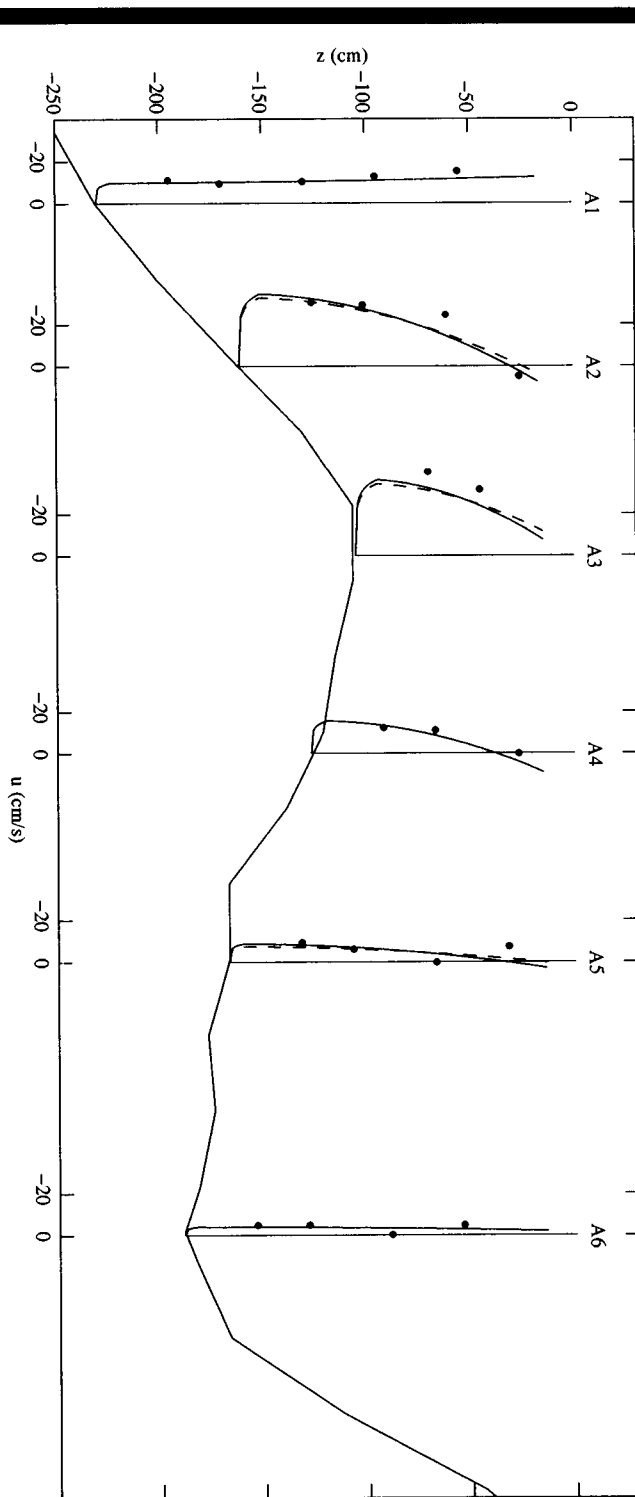


Figure 4. Model predictions for SSP92-A: Measured \bar{u} (\bullet); Predicted, Method 1 with adopted C_s (—); and Predicted, Method 1 with $C_{s,adv}$ (---).

zone to inside the surf zone is less pronounced for the irregular wave case. The magnitude of C_s is 0.1 which is much less than $(2/\pi) = 0.64$, indicating that (6) overpredicts the mean bottom shear stress as was found by COX and KOBAYASHI (1997). C_f generally decreases shoreward as was also noted in COX and KOBAYASHI (1997); however, C_f increases unexpectedly in the inner surf zone. Overall, the magnitude of C_f is on the order of 1.0, indicating that $\bar{f} \approx f_b$. Column 13 gives the values of C_u in (20) which are discussed later in relation to the prediction of the volume flux below trough level.

Figure 1 compares the model predictions with the measurements of SULTAN (1995). Trough level is indicated in the figure by the vertical extent of the model predictions. The horizontal extent from S1 to S12 is approximately 9 m. The figure indicates that the model predicts the measured undertow profile below trough level both outside and inside the surf zone for both methods with the coefficients adjusted at each measuring line. The boundary layer thickness is estimated by the model to be in the range $0.5 \leq \delta \leq 0.7$ cm, and the mean shear velocity is estimated to be in the range $-0.5 \leq \bar{u}_s \leq -0.2$ cm/s over the 12 measuring lines for Methods 1 and 2. These ranges indicate the difficulty in measuring the undertow and mean shear velocity in the bottom boundary layer in the laboratory. Figure 2 shows the model sensitivity to a 20% variation in C_s . In this figure, the adopted C_s at each measuring line is shown by a solid line whereas $0.8 C_s$ and $1.2 C_s$ are shown by dashed and dash-dot lines, respectively. A similar variation in the undertow profiles is achieved for only a 5% variation in C_f , and the figure is not shown for brevity.

Table 3 lists the input parameters to the model at each measuring line for the data of OKAYASU and KATAYAMA (1992). The local H_{rms} listed in Column 3 is estimated by $H_s = \sqrt{2}H_{rms}$ where the significant wave height H_s is estimated from the significant crest and trough elevations, $(\eta_c)_s$ and $(\eta_r)_s$, reported in OKAYASU and KATAYAMA (1992). Figure 3 compares the model and data for both methods. In this figure, the horizontal extent from O1 to O6 is approximately 5 m, and the triangular bar consists of three linear segments as explained in OKAYASU and KATAYAMA (1992). Figure 3 indicates that the model predicts the undertow profile over a barred bathymetry as well, apart from the scatter of data points at O6, provided that the coefficients are adjusted at each measuring line. For this case, the boundary thickness is estimated to be in the range $0.2 \leq \delta \leq 0.4$ cm, and the mean shear velocity is estimated to be in the range $-0.4 \leq \bar{u}_s \leq -0.05$ cm/s.

Table 4 lists the input parameters for Cases A, B, and C of the data of SMITH *et al.* (1992). The local H_{rms} value for each of the six measuring lines listed in these tables are obtained by a linear interpolation of the measured values in their paper. Although the local setup $\bar{\eta}$ was not measured, $\bar{\eta}$ was estimated in SMITH *et al.* (1992); and the ratio of this estimated setup to the minimum local water depth was approximately 0.03 for the three cases. Therefore, $\bar{\eta}$ is neglected here, and the approximation $\bar{h} \approx d$ is assumed for input in the undertow model. The trough level was also not reported, and the crude approximation of $\eta_{tr} \approx 0.3 H_{rms}$ is used here.

Table 6. Model input and calibration coefficients for HS94-A and HS94-B.

Line No.	d (cm)	H_{rms} (cm)	$\bar{\eta}$ (cm)	η_{tr} (cm)	Q_t (cm ² /s)	\bar{kh}	U_b (cm/s)	$A_b/k_s \times 10^{-5}$	$Re \times 10^{-2}$	f_b	C_*	C_f	C_u
A1	423	159	0.0	-48	-0.68	0.315	118	166	29	1.8	0.030	0.65	1.6
A2	359	146	0.0	-44	-0.57	0.290	118	166	29	1.8	0.030	0.63	1.5
A3	332	133	0.0	-40	-0.36	0.278	112	157	26	1.8	0.030	0.62	1.1
A4	300	114	0.0	-34	-0.47	0.264	101	143	22	1.9	0.030	0.60	1.8
A5	146	99	0.0	-30	-0.13	0.183	128	180	34	1.7	0.020	0.63	0.5
A6	93	71	0.0	-21	-0.17	0.146	115	162	28	1.8	0.030	0.61	1.1
A7	114	49	0.0	-15	-0.22	0.161	71	100	11	2.1	0.050	0.59	2.8
B1	418	139	0.0	-42	-0.48	0.289	103	158	25	1.8	0.030	0.63	1.4
B2	357	122	0.0	-37	-0.63	0.266	99	151	22	1.9	0.030	0.61	2.3
B3	332	96	0.0	-29	-0.44	0.256	80	123	15	2.0	0.030	0.61	2.4
B4	300	90	0.0	-27	-0.41	0.244	79	122	15	2.0	0.030	0.60	2.4
B5	200	101	0.0	-30	-0.13	0.198	111	169	28	1.8	0.020	0.63	0.5
B6	148	58	0.0	-17	-0.35	0.170	74	113	13	2.1	0.050	0.59	3.7
B7	159	47	0.0	-14	-0.26	0.177	58	88	8	2.3	0.040	0.59	4.2
B8	132	45	0.0	-14	-0.21	0.161	61	92	8	2.3	0.040	0.59	3.3

The relative roughness in (8) is found to be in the range $29 \leq A_b/k_s \leq 73$ for the three cases where the roughness height is assumed as $z_0 = 0.05$ cm and $k_s = 30 z_0 = 1.5$ cm for lack of data on bed forms. The Reynolds number is found to be in the range $2.1 \times 10^5 \leq Re \leq 7.8 \times 10^5$ for the field data. This range of relative roughness and Reynolds number indicates that the flow in the bottom boundary layer is rough turbulent even without the turbulence generated by wave breaking (JONSSON, 1966). The friction factor was found to be in the range $0.025 \leq f_b \leq 0.038$ which is larger than $f_b = 0.01$ specified in SMITH *et al.* (1992) for their model comparisons. However, the use of a much smaller value for z_0 would reduce f_b . For example, $z_0 = 0.007$ cm would yield the range $0.012 \leq f_b \leq 0.016$.

Table 4 shows that for a given case, C_* varies at each measuring line; but for a given measuring line, C_* is fairly constant for the three cases. Compared to the laboratory cases with regular waves (COX and KOBAYASHI, 1997), there is less cross-shore variation in C_* for a given case, although it is noted that the field measurements do not include the inner surf zone near the still water shoreline. The variation in C_f at a given measuring line for the three cases shown in Table 4 is also small. Table 5 lists the average values of C_* , C_p , and C_u for the six measuring lines. The values of C_* and C_f for these field data are smaller than the corresponding values of C_* and C_f listed in Tables 2 and 3 for the laboratory data. The mean shear velocity \bar{u}_* given by (7) and (16) depends on $C_f f_b$ and $C_f f_b$, respectively, instead of f_b itself. The calibrated values of C_* and C_f depends on the adopted value of z_0 which affects f_b somewhat, but the values of $C_f f_b$ and $C_f f_b$ remain approximately the same. In other words, the change of z_0 by a factor of 10 will change f_b , C_* , and C_f by roughly a factor of 2.

Figure 4 compares the undertow model for Method 1 with the data of SSP92-A using C_* listed in Table 4 and the average C_* values listed in Table 5. The horizontal extent from A1 to A6 is approximately 100 m. Figure 4 indicates that the model predicts the undertow profile over a barred beach for field conditions, provided that the coefficients are adjusted at each measuring line. The values of C_* are larger at A2 and A3 located immediately seaward and on the bar crest, re-

spectively, whereas the values of C_f do not change much across the barred beach. The agreement for Method 2 and for the two other cases SSP92-B and SSP92-C is similar, and the figures are not shown for brevity. For these field data, the boundary layer thickness is estimated to be in the range $4 \leq \delta \leq 11$ cm, and the mean shear velocity is estimated to be in the range $-2.1 \leq \bar{u}_* \leq -0.2$ cm/s. These values are much larger than the laboratory values estimated for S95 and OK92.

Table 6 lists the input parameters for comparisons with the data of HAINES and SALLENGER (1994). Similar to SMITH *et al.* (1992), $\bar{\eta}$ and η_{tr} were not given in the paper, and the assumptions of $\bar{h} \approx d$ and $\eta_{tr} \approx 0.3 H_{rms}$ are made here. The roughness height is assumed as $z_0 = 0.05$ cm, and the relative roughness is found to be in the range $88 \leq A_b/k_s \leq 180$. The Reynolds number is found to be in the range $8 \times 10^5 \leq Re \leq 34 \times 10^5$, indicating rough turbulent flow in the bottom boundary layer (JONSSON, 1966). Table 6 indicates that the cross-shore variations in C_* and C_f are small compared to the laboratory cases.

Figures 5 and 6 show the model agreement for HS94-A and HS94-B. The horizontal extent from A1 to A7 and from B1 to B8 is approximately 300 m. Substantial offshore migration of the bar occurred from October 11 (HS94-A) to October 12 (HS94-B) as explained in HAINES and SALLENGER (1994). The agreement is good for both methods and for both cases with the calibration coefficients adjusted at each measuring line. For these two cases, the boundary thickness is estimated to be in the range $11 \leq \delta \leq 17$ cm, and the mean shear velocity is estimated to be in the range $-1.5 \leq \bar{u}_* \leq -0.8$ cm/s. These ranges are similar to the field data of SSP92.

VOLUME FLUX BELOW TROUGH LEVEL

In the previous section, the volume flux below trough level has been specified using the measured volume flux at each measuring line. In this section, the local depth-averaged velocity \bar{U} is estimated using (20) with the measured values of H_{rms} and \bar{h} at the same location. The predictability of the depth-averaged velocity is discussed in terms of the calibra-

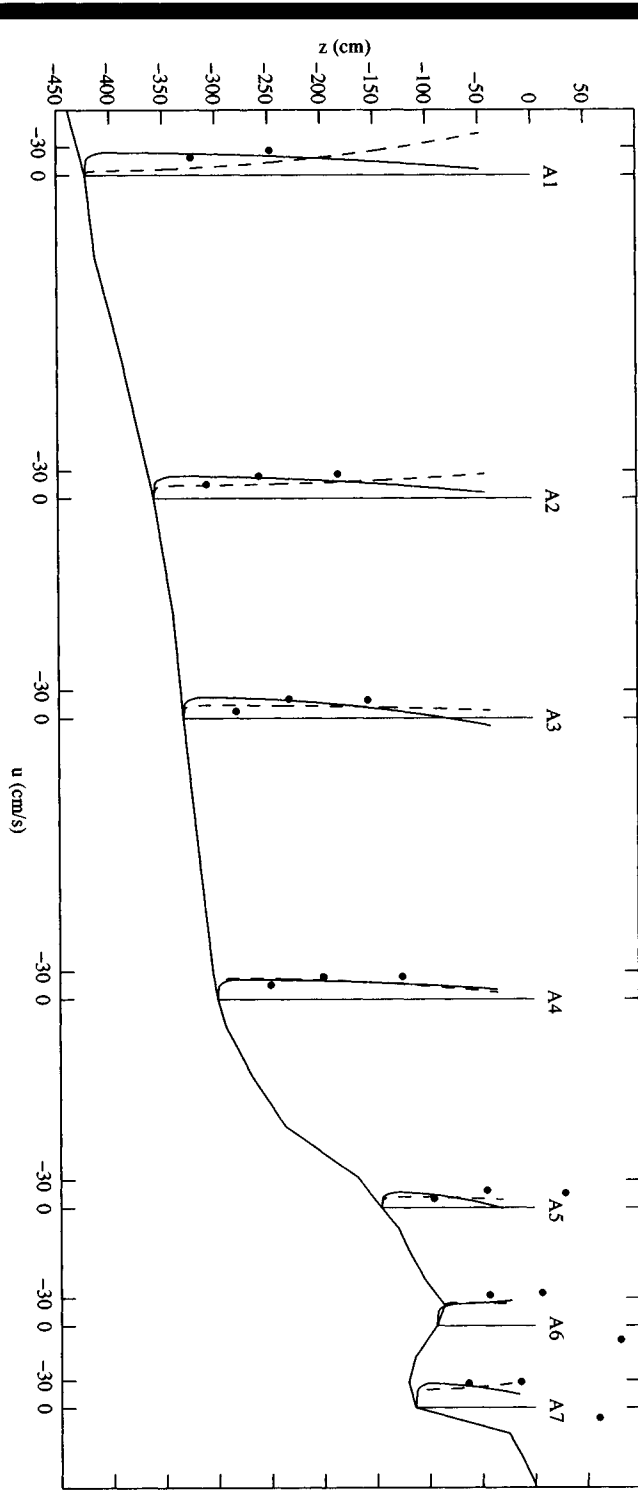


Figure 5. Model predictions for HS94-A: Measured \bar{u} (●); Predicted, Method 1 (—); and Predicted, Method 2 (---).

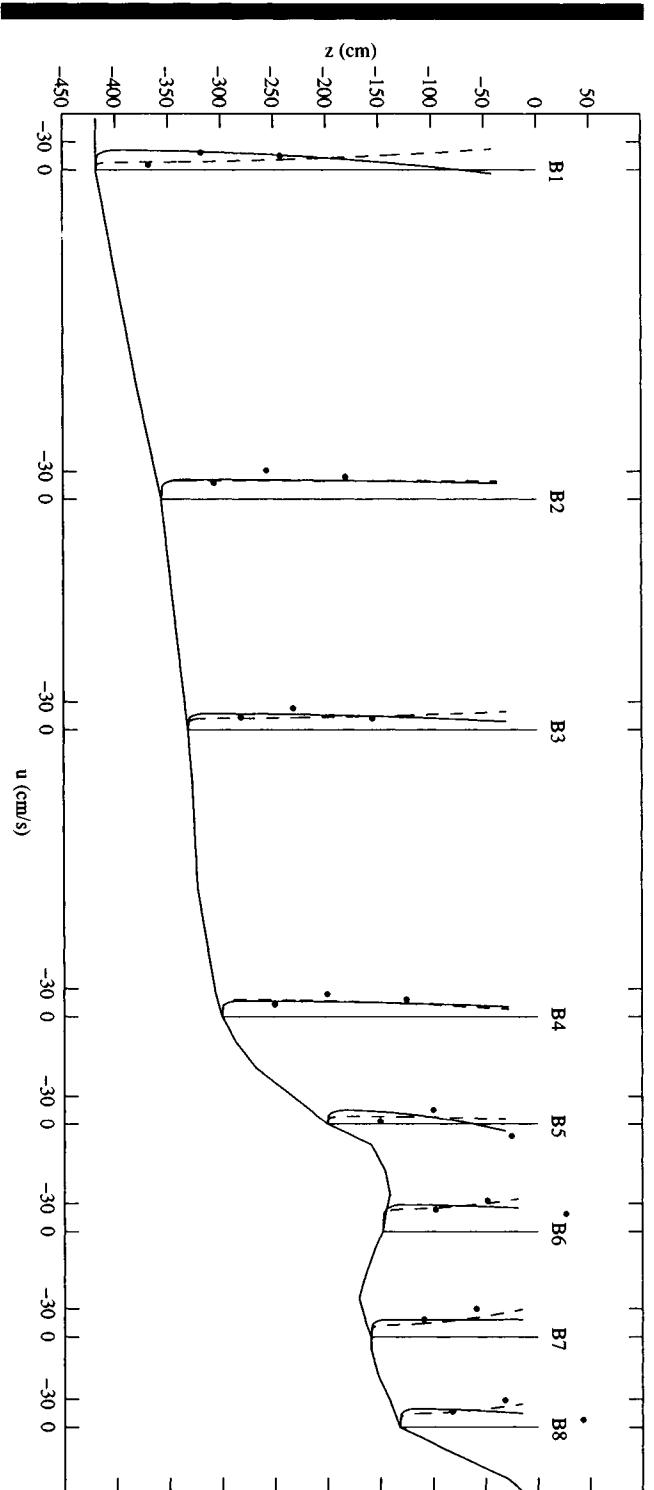


Figure 6. Model predictions for HS94-B: Measured \bar{u} (●); Predicted, Method 1 (—); and Predicted, Method 2 (---).

Table 7. Summary of calibrated values of $\overline{C_u}$.

Data Set	Outside Surf Zone		Breaker Zone		Bar/Trough Zone		Inner Surf Zone	
	Line	$\overline{C_u}$	Line	$\overline{C_u}$	Line	$\overline{C_u}$	Line	$\overline{C_u}$
S95	S1,S2	1.2	S3-S5	0.7	N/A ¹		S9-S12	2.1
OK92	O1	0.3	O2,O3	0.6	O4-O6	0.7		N/A ²
SSP92-A	A1	2.7	A2,A3	3.2	A4-A6	1.3		N/A ²
SSP92-B	B1	1.9	B2,B3	2.6	B4-B6	1.1		N/A ²
SSP92-C	C1	1.6	C2,C3	3.5	C4-C6	1.6		N/A ²
HS94-A	A1-A4	1.5	A5,A6	0.8	A7	2.8		N/A ²
HS94-B	B1-B4	2.1	B5	0.5	B6-B8	3.7		N/A ²

¹ Trough region not applicable to data of S95

² No inner surf zone measurements for these data sets

tion coefficient C_u which is obtained from (20) using the measured depth-averaged velocity given by $\overline{U} = (Q_r/d_{tr})$ together with the measured values of H_{rms} and \overline{h} . If the calibrated values of C_u are fairly constant, (20) may be applied to predict \overline{U} . Furthermore, the calibrated values of C_u can be used to assess the roller effect on C_u since $C_u = 1$ assuming no roller effect.

The calibrated values of C_u listed in Table 2 for S95 indicate that C_u is on the order of 1 over most of the shoaling and surf zone. For S9 to S12 in the inner surf zone, C_u is larger than 1, possibly due to the roller effect. The calibrated values of C_u for OK92 listed in Table 3 are generally less than 1. It is possible that the value of H_{rms} estimated from the significant crest and trough elevations reported by OKAYASU and KATAYAMA (1992) may not be very accurate. Noting that \overline{U} is proportional to H_{rms}^2 , this estimation error may have resulted in the unexpectedly small values of C_u for OK92.

On the other hand, the calibrated values of C_u in Tables 4 and 5 for the field data of SSP92 are mostly on the order of unity and tend to be larger over the bar crest region and smaller in the bar trough region in view of the measuring line locations shown in Figure 4. The calibrated values of C_u in Table 6 for HS94 are also on the order of unity for both cases, but C_u tends to be smaller for HS94-A which had a smaller longshore current than HS94-B.

Table 7 summarizes the calibrated values of C_u . The value $\overline{C_u}$ indicated in the table is estimated for each data set by averaging the C_u values over the measuring lines that have qualitatively similar locations in the cross-shore direction, namely outside the surf zone, the breaker zone, the bar-trough zone, and the inner surf zone. In general, Table 7 shows that $\overline{C_u}$ is closer to unity for the laboratory data sets

of S95 and OK92 than for the field data sets of SSP92 and HS94. There appears to be no systematic variation of $\overline{C_u}$ in the cross-shore direction as may be expected from the effect of rollers associated with regular breaking waves proposed by SVENDSEN (1984). For the irregular wave data in the laboratory, the roller effect is not very pronounced; and $C_u = 1$ is a reasonable approximation as has also been shown by KOBAYASHI *et al.* (1997). For the field data, $\overline{C_u}$ tends to be larger than unity, and the magnitude of the undertow velocities may have been modified by the wave directionality and alongshore variation of wave and current fields.

CONCLUSIONS

Existing undertow models based on a local balance of the horizontal momentum equation can predict the order magnitude of the undertow if empirical parameters are calibrated for each data set. Moreover, the literature is divided among regular or irregular waves and laboratory or field conditions with each model calibrated for one condition only. Rarely is it shown whether the empirical input is universal. For example, OKAYASU and KATAYAMA (1992) used empirically adjusted representative wave heights to get reasonable agreement with a model which was calibrated in an earlier paper under similar laboratory conditions. HAINES and SALLENGER (1994) employed a vertically uniform eddy viscosity which varied at each measuring line, and they attempted to parameterize this variation using their field data only.

Table 8 summarizes the types of data sets considered in this paper and in COX and KOBAYASHI (1997), listing the average calibration coefficients with the standard deviation given in parenthesis. These averages are crude in that they do not distinguish between areas of breaking and nonbreaking waves, but they serve to indicate the variability of the coefficients for the different data sets. Table 8 indicates that C_s and C_f are similar for both regular and irregular waves in the laboratories. For all of the data sets, Method 2 using C_f appears to be the most consistent in terms of the small standard deviation relative to the mean value. It was noted earlier in this paper and in COX and KOBAYASHI (1997), however, that the predicted undertow is more sensitive to small changes in the calibration coefficient C_f for Method 2 than C_s for Method 1.

The consistency of the average values of C_u between the two field data sets suggests that (20) with $C_u \approx 2$ might yield reasonable approximations of the depth-averaged undertow velocity \overline{U} , but the standard deviation is 1.1 and fairly large. The values of C_s and C_f for the field data tend to be smaller

Table 8. Summary of calibration coefficients.

Literature Cited	Lab or Field	Wave Condition	Bathymetry	C_s	C_f	C_u
Sultan (1995)	Lab	Irregular	Plane, smooth	0.09 (.04)	1.0 (.2)	1.3 (.8)
Okayasu and Katayama (1992)	Lab	Irregular	Barred, smooth	0.06 (.02)	1.4 (.4)	0.6 (.3)
Smith <i>et al.</i> (1992)	Field	Irregular	Barred, rough	0.03 (.02)	0.22 (.01)	2.0 (1.1)
Haines and Sallenger (1994)	Field	Irregular	Barred, rough	0.03 (.01)	0.61 (.02)	2.0 (1.1)
Cox <i>et al.</i> (1995)	Lab	Regular	Plane, rough	0.05 (.03)	0.47 (.04)	—
Hansen and Svendsen (1984)	Lab	Regular	Plane, smooth	0.10 (.04)	1.0 (.3)	—
Nadaoka and Kondoh (1982)	Lab	Regular	Plane, smooth	0.10 (.05)	0.9 (.2)	—

than those for the laboratory data, but these values of C_s and C_f are affected somewhat by the adopted value of z_0 as explained in relation to Table 4 as well as by the presence of longshore currents. Furthermore, errors associated with use of the model where the volume flux and calibration coefficients are not known are approximately 100% or roughly a factor of 2.

Finally, the values of C_s for all the data sets in Table 8 are definitely less than $C_s = (2/\pi) = 0.64$ based on (6). Consequently, (6) overpredicts the mean bottom shear stress. The alternative equation (16) with $\bar{f} = C_f f_b$ has been proposed by COX and KOBAYASHI (1997) to mitigate the shortcomings of (6), but (16) is physically unsatisfactory because it neglects wave effects. Therefore, it may be concluded that the mean cross-shore bottom shear stress is poorly understood. The state of the art for the alongshore bottom shear stress in the surf zone is similar (CHURCH and THORNTON, 1993).

ACKNOWLEDGEMENTS

The authors thank the reviewer for his comments. This work was partially sponsored by the U.S. Army Research Office, University Research Initiative under contract No. DAAL03-92-G-0116 and by the National Science Foundation under grant No. CTS-9407827.

LITERATURE CITED

- BATJES, J.A., 1974. Surf similarity. *Proc. 14th International Conference on Coastal Engineering* (ASCE), pp. 466–479.
- BATJES, J.A. and JANSSEN, J.P.F.M., 1978. Energy loss and set-up due to breaking of random waves. *Proc. 16th Int. Conf. on Coast. Engrg.* (ASCE), pp. 569–587.
- BATJES, J.A. and STIVE, M.J.F., 1985. Calibration and verification of a dissipation model for random breaking waves. *Journal Geophysical Research*, 90(C5), 9159–9167.
- CHURCH, J.C. and THORNTON, E.B., 1993. Effects of breaking wave induced turbulence within a longshore current model. *Coastal Engineering*, 20, 1–28.
- COX, D.T. and KOBAYASHI, N., 1996. Undertow profiles in the bottom boundary layer under breaking waves. *Proc. 25th Int. Conf. on Coastal Engrg.*, (ASCE), 3, 3194–3206.
- COX, D.T. and KOBAYASHI, N., 1997. A kinematic undertow model with a logarithmic boundary layer. *Journal Waterway, Port, Coastal, and Ocean Engineering* 123 (6), 354–360.
- COX, D.T.; KOBAYASHI, N., and OKAYASU, A., 1996. Bottom shear stress in the surf zone. *Journal Geophysical Research*, 101 (C6), 14337–14348.
- DALLY, W.B. and DEAN, R.G., 1984. Suspended sediment transport and beach evolution. *Journal Waterway, Port, Coastal, and Ocean Engineering*, 110 (1), 15–33.
- GRANT, W.D. and MADSEN, O.S., 1979. Combined wave and current interaction with a rough bottom. *J. Geophysical Research*, 84 (C4), 1797–1808.
- GRANT, W.D. and MADSEN, O.S., 1986. The continental shelf bottom boundary layer. *Annual Reviews Fluid Mechanics*, 18, 265–305.
- HAINES, J.W. and SALLENGER, A.H., 1994. Vertical structure of mean cross-shore currents across a barred surf zone. *J. Geophys. Res.*, 99 (C7), 14223–14242.
- HANSEN, J.B. and SVENDSEN, I.A., 1984. A theoretical and experimental study of undertow. *Proc. 19th Int. Cont. on Coastal Engrg.*, ASCE, 2246–2262.
- JONSSON, I.G., 1966. Wave boundary layers and friction factors. *Proc. 10th Int. Conf. on Coastal Engrg.*, ASCE, 127–148.
- KAMPHUIS, J.W., 1975. Friction factor under oscillatory waves. *J. Waterway, Harbors and Coastal Engrg.*, 101 (2), 135–144.
- KOBAYASHI, N.; HERRMAN, M.N.; JOHNSON, B.D., and ORZECH, M.D., 1998. Probability distribution of surface elevations in surf and swash zones. *J. Waterway, Port, Coastal, and Ocean Engrg.*, 124, (3), 99–107.
- KOBAYASHI, N. and KARJADI, E., 1996. Obliquely incident irregular waves in surf and swash zones. *J. Geophys. Res.*, 101 (C3), 6527–6542.
- NADAOKA, K. and KONDOH, T., 1982. Laboratory measurements of velocity field structure in the surf zone by LDV. *Coastal Engrg. in Japan*, 25, 125–145.
- NIELSEN, P., 1992. *Coastal Bottom Boundary Layers and Sediment Transport*. River Edge, New Jersey: World Scientific, 324p.
- OKAYASU, A. and KATAYAMA, H., 1992. Distribution of undertow and long-wave component velocity due to random waves. *Proc. 23rd Int. Conf. on Coastal Engrg.*, (ASCE) 883–893.
- ROELVINK, J.A. and BROKER, I., 1993. Cross-shore profile models. *Coastal Engrg.*, 21, 163–191.
- SMITH, J.M.; SVENDSEN, L.A., and PUTREVU, U., 1992. Vertical structure of the nearshore current at DELILAH: Measured and modeled. *Proc. 23rd Int. Conf. on Coastal Engrg.*, (ASCE) 2825–2838.
- SCHLICHTING, H., 1979. *Boundary-Layer Theory*, New York: McGraw-Hill, 817p.
- STIVE, M.J.F. and WIND, H.G., 1986. Cross-shore mean flow in the surf zone. *Coastal Engrg.*, 10, 325–340.
- SULTAN, N., 1995. Irregular Wave Kinematics in the Surf Zone. Ph.D. Dissertation, Texas A&M University, College Station, Texas.
- SVENDSEN, I.A., 1984. Mass flux and undertow in a surf zone. *Coastal Engrg.*, 8, 247–365.
- SVENDSEN, I.A.; SCHÄFFER, H.A., and HANSEN, J.B., 1987. The interaction between the undertow and the boundary layer flow on a beach. *J. Geophys. Res.*, 92 (C11), 11845–11856.
- THORNTON, E.B.; HUMISTON, R.T., and BIRKEMEIER, W., 1996. Bar/trough generation on a natural beach. *J. Geophys. Res.*, 101 (C5), 12097–12110.